Journal of Sustainable Cement-Based Materials

ISSN: (Print) (Online) Journal homepage: www.tandfonline.com/journals/tscm20

Carbonation of calcium sulfoaluminate belite binder: mechanism and its implication on properties

Vaishnav Kumar Shenbagam, Paul Shaji, Yakkala Eswita, Rolands Cepuritis & Piyush Chaunsali

To cite this article: Vaishnav Kumar Shenbagam, Paul Shaji, Yakkala Eswita, Rolands Cepuritis & Piyush Chaunsali (23 Jan 2024): Carbonation of calcium sulfoaluminate belite binder: mechanism and its implication on properties, Journal of Sustainable Cement-Based Materials, DOI: 10.1080/21650373.2024.2306271

To link to this article: https://doi.org/10.1080/21650373.2024.2306271

Journal of Sustainable Cement-Based Materials, 2024
http://dx.doi.org/10.1080/21650373.2024.2306271

Carbonation of calcium sulfoaluminate belite binder: mechanism and its implication on properties

Vaishnav Kumar Shenbagam[a], Paul Shaji[a], Yakkala Eswita[a], Rolands Cepuritis[b] and Piyush Chaunsali[a]*

[a]*Department of Civil Engineering, Indian Institute of Technology Madras, Chennai, India;* [b]*Department of Structural Engineering, Norwegian University of Science and Technology, Trondheim, Norway*

Calcium sulfoaluminate belite (CSAB) binder is an alternative low CO_2 binder. CSAB cement has ye'elimite as the primary clinker phase which hydrates to form monosulfate or ettringite as the main hydration product. The hydration and mechanical characteristics of CSAB cement and PC-CSAB blended cement have been reported in several studies; however, studies on the durability characteristics such as carbonation are limited. This study focuses on evaluating the microstructural and mechanical alterations due to carbonation in a CSAB binder system and understanding the underlying mechanism of development of the carbonation front. CSAB binder was found to carbonate rapidly compared to PC binder, accompanied by a reduction in compressive strength. This was attributed to the increase in the pore volume due to the carbonation of the ettringite-rich microstructure, facilitating further ingress of CO_2 into the microstructure. The rate of carbonation in CSAB binders diverged significantly from the square root of time model used for PC binders.

Keywords: Calcium sulfoaluminate belite cement; Ye'elimite; ettringite; carbonation; pore structure

1. Introduction

Calcium sulfoaluminate belite (CSAB) cement is an alternative low CO_2 binder, with a reduced carbon footprint than conventional Portland Cement (PC) [1–4]. The research interest in CSAB cement is increasing as there is a drive to reduce the carbon footprint of cement and concrete [5,6]. The reduction in CO_2 emissions can be attributed to the presence of ye'elimite ($C_4A_3\hat{S}$) as the primary phase in CSAB cement, which has a lower limestone requirement and is formed at 1200 °C, which is lower than the temperatures required for the formation of PC clinker phases (1450-1500 °C) [7]. The hydrated phase assemblage of CSAB cement differs significantly from that of PC [8–10].

Ye'elimite, the primary phase of CSAB cement, reacts rapidly to form a dense microstructure resulting in high early-age strength and rapid hardening [11,12]. The hydration of belite may occur at later ages leading to the formation of C-S-H gel or strätlingite [13,14]. Although there are several studies on the hydration and mechanical characteristics of CSAB cement, the literature available on durability characteristics such as corrosion resistance [15–17], carbonation resistance [18–23] and chemical resistance [24,25] are limited.

Carbonation resistance of a binder is important for durability of reinforced concrete as the ingress and reaction of atmospheric CO_2 with the cementitious phases reduces the pH of pore solution in the binder. The reduction in pH of pore solution directly affects the passivation of steel and the stability of hydrated phases leading to a reduction in the service life of the structure [26]. The carbonation in cementitious systems can be seen as a two-stage process: first, the diffusion of CO_2 into the binder matrix, and second, the reaction of CO_2 with the hydrated cement phases [27]. The carbonation resistance can be evaluated based on the rate at which the depth of carbonated region progresses. The depth of carbonation at a particular age or the carbonation coefficient of binder system can be used as a parameter to compare different binders. Tuutti's square root of time model determines the carbonation coefficient as per the following Equation 1 and is based on the Fick's law of diffusion [28].

$$d_{CO2} = K_{CO2}.t^{0.5} \tag{1}$$

The rate of carbonation is influenced by the binder properties and the external environment. The physico-chemical characteristics of binders, such as the amount of carbonatable content, buffering capacity of the hydrated phases, pH of pore solution, internal humidity, and pore structure characteristics, will have a significant impact on their carbonation resistance [29–31]. In CSAB cement, the main hydration product ettringite decomposes to form gypsum, aluminum hydroxide, and calcium carbonate on exposure to CO_2 (Equation 4). The monosulfate phase in the presence of CO_2 initially converts into ettringite and carboaluminate phase, which eventually converts into gypsum, aluminum hydroxide, and calcium carbonate (Equations 2–4) [19].

$$6C_3A.C\hat{S}.12H + 3\ H\hat{C} + 25\ H \rightarrow 2C_3A.3C\hat{S}.32H + 3C_3A.C\hat{C}.H_{11} + AH_3 \tag{2}$$

$$C_3A.C\hat{C}.H_{11} + 3H\hat{C} \rightarrow 4C\hat{C} + AH_3 + 11H \tag{3}$$

$$C_3A.3C\hat{S}.32H + 3H\hat{C} \rightarrow 3C\hat{C} + AH_3 + 3C\hat{S}H_2 + 26H \tag{4}$$

(According to cement chemistry notation: C = CaO; A = Al_2O_3; S = SiO_2; $\hat{S}$ = SO_3; F = Fe_2O_3; H = H_2O; C^a = CO_2)

*Corresponding author. Email: pchaunsali@iitm.ac.in

The literature on carbonation resistance of CSAB cement is conflicted. The earlier works on the carbonation resistance of CSAB cement from the service structures reported good carbonation resistance of CSAB cement compared to [23, 32,33]. Whereas the recent studies on paste/mortar have reported have reported a poorer carbonation resistance of CSAB cement compared to PC in laboratory scale [15, 19, 21, 34,35]. When we compare the parameters that influence the carbonation resistance of a binder, CSAB cement has a lower CO_2 binding capacity or carbonatable content than PC. In the absence of portlandite (which acts as pH buffer in PC), ettringite phase in CSAB cement is attacked and carbonated first. However, a denser pore structure and reduced relative humidity (RH) in CSAB binder matrix (due to self-desiccation) can help reduce the rate of diffusion of CO_2 [19, 36]. Further carbonation and decomposition of ettringite has been reported to increase the pore volume and decrease the compressive strength [17, 19, 21, 37]. The study by [19] indicated that the carbonation resistance of CSAB cements increased with the $C\hat{S}:C_4A_3\hat{S}$ ratio [19]. Whereas in another study [18], reported a reduction in the carbonation resistance with loss in strength with the addition of calcium sulfate [18]. Although the studies reported a change in the carbonation resistance with the addition of calcium sulfate, the effect of calcium sulfate on microstructural characteristics was not fully considered in the study. The addition of calcium sulfate can also affect the other properties such as reducing the pH of the pore solution, which will have an effect on the carbonation resistance. Thus, a comprehensive study is needed to understand the carbonation resistance of CSAB cement and the changes at both microstructural level and the macro-mechanical properties.

The current work examines a CSAB cement (forming monosulfate and ettringite) and a gypsum-blended CSAB cement (ettringite rich) to examine the effect of carbonation-induced changes on their mechanical properties. This study also draws a comparison of these binders to PC and PC-CSAB* (CSAB admixture) blended system. A detailed physico-chemical characterization of control (hydrated) and carbonated sample was performed to understand the mechanism of the evolution of carbonation front in these ettringite-rich CSAB binder systems.

2. Materials

The raw materials used in this study were based on two different binder systems, a Portland cement of Grade 53 as per IS 269 (denoted as PC henceforth), a commercially available calcium sulfoaluminate belite binder (denoted as CSAB henceforth). These binders were additionally blended with a commercially available calcium sulfoaluminate belite admixture (denoted as CSAB* henceforth), and a laboratory-grade calcium sulfate dihydrate (gypsum), which can potentially make the PC and CSAB binders expansive (by increasing the amount of ettringite), respectively [38–40]. The phase compositions of different binders as determined using quantitative X-ray diffraction (QXRD) are provided in Table 1. The cement paste specimens were cast using distilled water. For the cement mortar samples, standard sand was used. Table 2 shows various binder systems and corresponding water-to-binder (w/b) ratios. The binder systems can be broadly grouped as PC dominant system (PC and PC-CSAB* blended cement) and CSAB dominant system (CSAB and CSAB_$\hat{S}$ binder). The addition of gypsum to CSAB will increase the molar ratio of calcium sulfate-to-ye'elimite (*M-value*) over 2 (the theoretically required amount of calcium sulfate to convert ye'elimite to ettringite completely, based on stoichiometry), so as to avoid the formation of monosulfate and have an ettringite-rich system. PC-based binders (PC and PC_CSAB*) had w/b of 0.4, whereas CSAB binders had w/b of 0.5. Due to the difference in water demand of two binder systems (PC based and CSAB based), different w/b ratios were selected. Also, based on preliminary studies, it was found that the four binder combinations required different w/b ratios to attain an equivalent compressive strength of 30 ± 2 MPa at 7 days, thus enabling comparison of carbonation resistance of binders at similar strength levels.

Table 1. Phase composition of binders calculated from QXRD (%wt.).

Phases	PC	CSAB*	CSAB
Alite	48.8	0	0
Belite	28.2	9.9	24.9
Tricalcium aluminate	6.4	0	3.9
Tetracalcium aluminoferrite	8.5	1.2	0
Ye'elimite	0	14.0	45.2
Anhydrite	0	43.0	14.9
Lime	0	21.1	0
Mayenite	0	3.1	0
Gypsum	1.9	0	2.5
Dolomite	0	5.5	6.0
Calcite	3.9	0	0
Quartz	<2%	0	<2%
Portlandite	<2%	<2%	0

Table 2. Mixture proportions of different binder systems (%wt.).

Nomenclature	PC	CSAB*	CSAB	Gypsum	w/b
PC	100	0	–	–	0.4
PC_CSAB*	90	10	–	–	0.4
CSAB	–	–	100	0	0.5
CSAB_$\hat{S}$	–	–	85	15	0.5

3. Experimental methods

3.1. Sample preparation

All the materials were pre-conditioned for at least 24 h before casting at an environment of $25\,^{\circ}C \pm 2\,^{\circ}C$. The cement paste samples and mortar samples were mixed using a planetary Hobart mixer, cast and cured under the same temperature-controlled environment. Cement paste samples for characterisation studies were prepared separately and cut into 2–3 mm thin slices at the required age(s). This was followed by hydration stoppage using

using isopropyl alcohol (IPA). All the samples were then dried and stored in a vacuum desiccator until testing.

3.2. Carbonation depth

Carbonation depth was monitored in prismatic specimens of cement paste (cross section: 25 mm × 25 mm) and mortar (cross section: 40 mm × 40 mm) under natural and accelerated (3% CO_2) environments. The prismatic specimens were conditioned for 7 days at 65% RH after the initial curing period before they were subjected to either a natural or accelerated (concentration of 3% CO_2) environment at 65% RH. Similarly, cement mortar cubes were also conditioned and exposed to an accelerated CO_2 environment to assess the influence of carbonation on compressive strength. The cement paste specimens were cured (100%RH and 25 °C) for two different durations of 7 and 28 days (denoted as Paste_7 and Paste_28, respectively) and the cement mortar specimens were cured (100%RH and 25 °C) for 28 days (denoted as Mortar_28). The two different curing durations were selected to observe the effect of pore structure on the carbonation resistance, as binder cured for a longer duration (28 days) would have a denser pore structure. The depth of carbonation was measured at regular intervals by breaking the specimens through shearing and spraying phenolphthalein indicator on exposed surface. The carbonated layer was distinguished from the uncarbonated zone based on the colour change. The pink coloured region represented the zone of uncarbonated sample having higher pH than carbonated zone. The cross-section images were captured, and the depth of carbonation was determined using an image processing software by averaging at 12 locations across all sides.

3.3. Physical characteristics

Compressive strength was measured using mortar specimens of size 50 mm × 50 mm × 50 mm. In order to understand the effect of carbonation on compressive strength, one set of mortar cubes (age: 28 days) were wrapped using polyethylene cling wraps (control) and one set of mortar cubes (age: 28 days) were exposed to an accelerated CO_2 environment and tested after 28 days of exposure. The compressive strength was determined by testing the cubes in a universal testing machine under a loading rate of 1460 N/s.

The changes in the pore structure features were characterised using the oxygen permeability index (OPI) test and mercury intrusion porosimetry (MIP). OPI test was performed on cement mortar specimens and MIP was performed on cement paste samples. Cement mortar specimens (70 mm diameter and 30 mm thickness) were obtained by coring from a 100 mm cement mortar cube. The specimens were conditioned at 50 °C in an oven for 7 days and coated with epoxy on the side surface before testing. The permeability was tested on a falling head permeability cell with 100 kPa pressure as per the South African Durability Index manual [41]. The negative logarithm of Darcy's permeability coefficient was represented as the OPI value. As this was a non-destructive test, the samples were exposed to an accelerated CO_2 environment and tested post-carbonation. MIP test was performed using a two stage ThermoScientific Pascal 140-440 instrument. The cement paste sample of about 1 g was collected from the hydrated and carbonated specimen and tested. The sample was tested in the pressure range of 0–100 kPa and 0.1–300 MPa at the rate of 6 kPa/s and 6 MPa/s, respectively. The pressure was converted to the corresponding pore size using the contact angle and the surface tension values of 140° and 0.48 N/m, respectively.

Dimensional changes were monitored to capture the effect of carbonation, if any. Cement paste prisms of size 25 mm × 25 mm × 285 mm were cast with a stud gauge fixed at the ends and the dimensions were monitored regularly against an standard invar bar used as the reference. The change in dimension was recorded with reference to the first reading at 24 h after demoulding. The specimens were cured (100%RH and 25 °C) for 7 days followed by exposure to a drying environment at 65% RH or 3% accelerated CO_2 environment. The average change in dimension of the three specimens was recorded with time.

3.4. Chemical characterisation

The evolution of hydrated phase assemblage during curing and after carbonation was studied using quantitative X-ray diffraction (QXRD) and thermogravimetric analysis (TGA). The samples after hydration stoppage were ground using an agate mortar pestle and sieved through a 75 μm sieve to be used for testing. X-ray diffractograms were collected using a MiniFlex Rigaku benchtop powder X-ray diffraction instrument having CuKα radiation (wavelength of 1.5405 Å) generated at 45 kV and 15 mA. The scanning parameters used were: 2-Theta (2θ) range of 5°–60°; step size of 0.02° and scanning rate of 10°/min. The samples were also blended with known quantities (20% by wt.) of ZnO which was used as an internal standard before testing. The diffractograms were analysed using X'Pert HighScore Plus for quantitative analysis using Rietveld refinement.

TGA was performed using an SDT 650 Simultaneous thermal analyser from TA Instruments. The samples were heated from a temperature of 30 °C to a maximum temperature of 900 °C at a heating rate of 15 °C/min under a nitrogen-purged environment.

The pH measurements were carried out by extracting the pore solution from cement paste samples. The pore solution was extracted at the required ages by loading the samples under triaxial compression to 800 kN at a loading rate of 2000 N/s [42]. The maximum load was maintained for a period of 5 min to allow for the solution to drain into the container. The pore solution collected was filtered through a 0.20 micrometre syringe filter a part of the solution was immediately tested for pH. Alternatively, powdered cement paste sample was diluted in deionised water to check the pH of the samples at later ages. This method was used to determine the pH at later ages (28 days) in the carbonated sample as extracting pore solution would not be practicable at later ages. The pH measurements were

made using a pH electrode and pH meter manufactured by Metrohm connected which was calibrated using 3 point calibration standard calibration solutions.

The changes in the hydrated phase assemblage under carbonation was also modelled and predicted using a geochemical modelling software, GEMS. The thermodynamic modelling was performed using GEM-Selektor v.3 [43–45] using cement specific data (Cemdata18.1) [46]. The initial phase composition (from XRD) of the binder was used as the input to the system by manually controlling the reactive phases. Further, the hydrated phases such as gibbsite that are not generally found in the CSAB hydrated system were added manually. The GEMS modelling was performed using at the w/b ratio of 1.0 for the system to have sufficient water for the equilibrium reactions.

4. Results and discussion

4.1. Carbonation depth under natural and accelerated carbonation environments

Carbonation of CSAB binder system was monitored and compared against PC binder system by exposing the specimens to either natural or accelerated carbonation environments. The depth of carbonation was captured by tracking the pH change across the cross section of specimen as the ingress of CO_2 is associated with pH reduction. The carbonated region could be identified using a phenolphthalein indicator. The intensity of colour change (with respect to pink in the uncarbonated zone) was observed to be lesser in CSAB binder than in PC binder systems (Figure 1). The reduced intensity could be due to the lower pH in CSAB binders. The colour change was, however, sufficient to distinguish the carbonated region.

The change in carbonation depth of the CSAB paste (cured for 7 days and exposed to 3% CO_2 environment) is shown in Figure 2. It is evident that the CSAB binder carbonated completely by 28 days. The CSAB specimens were also observed to have bands or zones which resemble the Liesegang patterns observed in carbonated lime mortar [47]. The rapid progression of the carbonation front could be one of the reasons for the formation of these patterns; however, further investigation is required to understand the formation of these bands.

The progression of carbonated layer under accelerated and natural environments for the cement paste and mortar specimens is shown in Figure 3. CSAB binder had the highest rate of carbonation, which was reduced with the addition of gypsum (as in CSAB_$\hat{S}$ binder). A similar trend was observed in both natural and accelerated carbonation environments. Whereas in PC binder systems (PC and PC_CSAB*), a visible presence of carbonated region was observed only after about 56 days of exposure to accelerated carbonation environment. As the PC based binder systems did not carbonate sufficiently, the progression of carbonation front has not been included in the plots. Difference in hydrated phase assemblages and w/b ratios of PC and CSAB binders could be affecting the carbonation resistance. The carbonation resistance of CSAB binder was enhanced with the addition of gypsum as the depth of carbonation was reduced by over 25% when 15% gypsum was blended with CSAB binder in paste samples cured for 7 days. A similar effect was observed when the addition of calcium sulfate enhanced the hydration kinetics of ye'elimite and improved the carbonation resistance [19]. However, the enhancement of carbonation resistance was less than 10% in the paste samples cured for 28 days. Similarly, the improvement was over 25% in cement mortars. The addition of gypsum to CSAB cement alters the hydration kinetics, hydrated phase assemblage and the pore structure characteristics [40], which could lead to the enhancement of carbonation resistance. Furthermore, mechanical, and microstructural characterisation studies were conducted to evaluate to the effect of carbonation. As the PC binder systems did not carbonate significantly, only the CSAB binder systems were considered for the microstructural characterisation to observe the changes upon carbonation.

4.2. Changes in the chemical characteristics

4.2.1. Hydrated phase assemblage of CSAB binder system on carbonation: XRD

Phase assemblage of hydrated cement paste samples was determined after a curing period of 7 days and 28 days. In order to understand the change in phase composition after carbonation, the cement paste samples (after curing for 7 days and 28 days) were powdered and placed in a 3% CO_2 environment for 28 days to ensure complete carbonation. Figures 4 and 5 show the changes in the hydrated phase assemblage of CSAB binders (CSAB and CSAB_$\hat{S}$) due to carbonation.

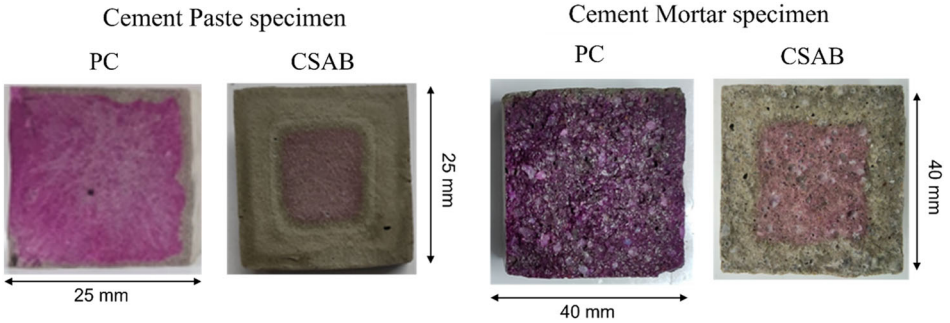

Figure 1. Colour change observed in PC and CSAB binders on spraying with a phenolphthalein indicator to distinguish the carbonated region (Left: Cement paste specimen after 14 days of exposure, Right: Cement mortar specimen after 28 days of exposure).

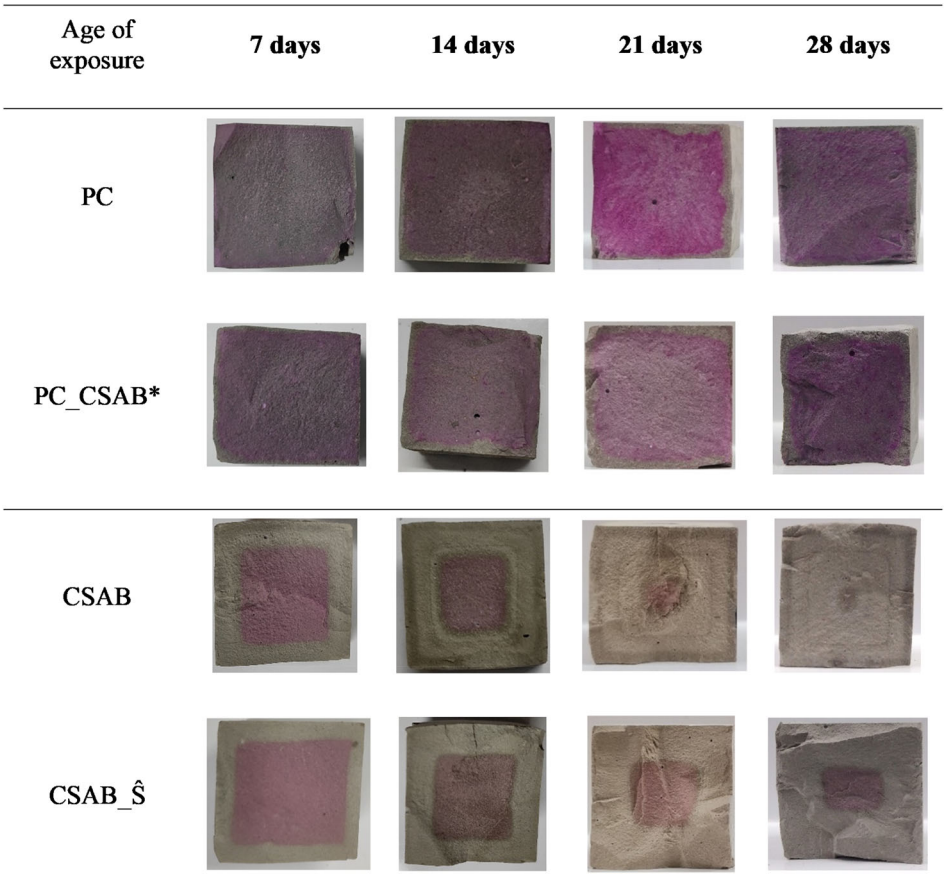

Figure 2. Progression of carbonation in the different binder system in cement paste specimen cured for 7 days and subjected to accelerated carbonation at 3% CO_2.

CSAB binders have prominent peaks of ettringite phase – the main hydration product. The aluminium hydroxide phase was not detected in XRD as it could be microcrystalline or amorphous. There was also a presence of ye'elimite peak in CSAB binder at 7 and 28 days, which could indicate the lack of sulfate source or water for the complete hydration. A similar result was reported in literature, where ye'elimite in the absence of sufficient sulfate source did not form monosulfate, but remained unreacted [48]. In CSAB_Ŝ binder with the addition of sulfate source, ye'elimite was completely consumed. In both CSAB and CSAB_Ŝ binders, there was no significant reaction of belite observed at 7 and 28 days. Lack of sufficient water could be a reason for belite to remain unreactive till 28 days. Upon carbonation, the ettringite peak diminished completely in all samples, and there was also a corresponding increase in the intensity of gypsum peak. Additionally, the presence of calcium carbonate was found to be in the form of calcite and aragonite (two polymorphs of calcium carbonate). Although the calcite phase is usually expected from the carbonation of hydrated cement systems, the formation of aragonite could be due to the higher rate of carbonation. Similar co-existence of calcium carbonate in the form of calcite and aragonite has also been reported in the literature [49,50]. There was also an increase in the amorphous content, which could be attributed to the formation of aluminium hydroxide from the decomposition of ettringite. In all the carbonated samples, the peak for belite was not present, indicating its carbonation as there was no evidence of belite hydration till 28 days. The carbonation of ettringite phase is accompanied with the release of high amount of water (over 50% by wt.) according to Equation 4, which can facilitate the hydration of belite and further carbonation to form calcium carbonate and amorphous silica. The phase composition of hydrated and carbonated samples quantified using XRD is shown in Table 3. The carbonated samples were found to have over 10% (by wt.) of carbonate phases. The conversion of 30% of ettringite can only contribute to about 7% (by wt.) of calcium carbonate phases (as per Equation 4), which further shows the contribution of belite phase toward the carbonated phases.

4.2.2. Change in the hydrated phase assemblage due to carbonation: TGA

Figure 6 shows differential thermogravimetric analysis of the hydrated and carbonated CSAB binder. The hydrated CSAB binder had predominantly ettringite along with aluminium hydroxide. In the carbonated sample, gypsum and aluminium hydroxide were observed in addition to calcium carbonate, which was absent in the hydrated sample. The carbonated sample also had a bimodal peak near 100 °C; this could indicate the presence of amorphous phases (not detectable in XRD) such as C-S-H gel from the hydration of belite or amorphous ettringite. However, further tests need to be performed to confirm the presence of these phases.

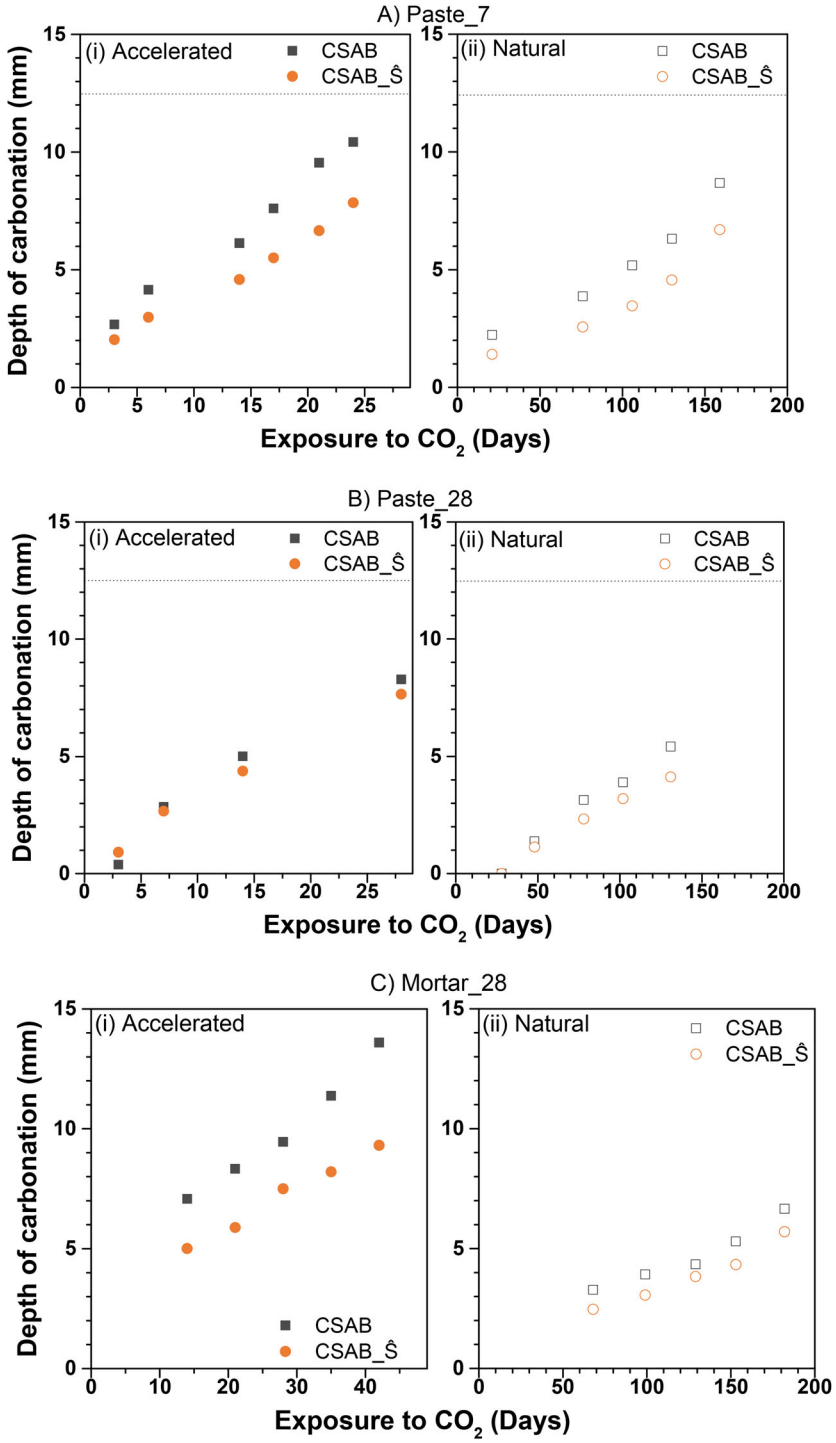

Figure 3. Depth of carbonation in CSAB mortar specimen under accelerated and natural carbonation of a) cement paste exposed after 7 days of curing; b) cement paste exposed after 28 days of curing; and c) cement mortar exposed after 28 days of curing.

4.2.3. Effect of carbonation on the pH of pore solution

The pH of binder was measured by extracting its pore solution. The pH of pore solution of CSAB binder at 1 day was 12.05. CSAB binders typically have lower pH than PC [14]. The addition of gypsum further reduced the pH of the pore solution (Table 4). Although ettringite has been reported to be unstable at low pH levels, ettringite was the main and stable hydration product formed in CSAB_ Ŝ binder having pH of 9.64. Similarly, the powder sample was also used to check the change in pH of the hydrated and the carbonated samples. The difference in the pH values (at 1 day and 28 days) could be partly due to continued hydration and also partly attributed to different methods used in determining the pH. However, there is a clear decrease in the pH of the samples after carbonation, both the binders had low pH (less than 9) after carbonation. The reduction in pH levels below 9 could also be a factor contributing to the rapid disintegration of ettringite in CSAB binders on carbonation.

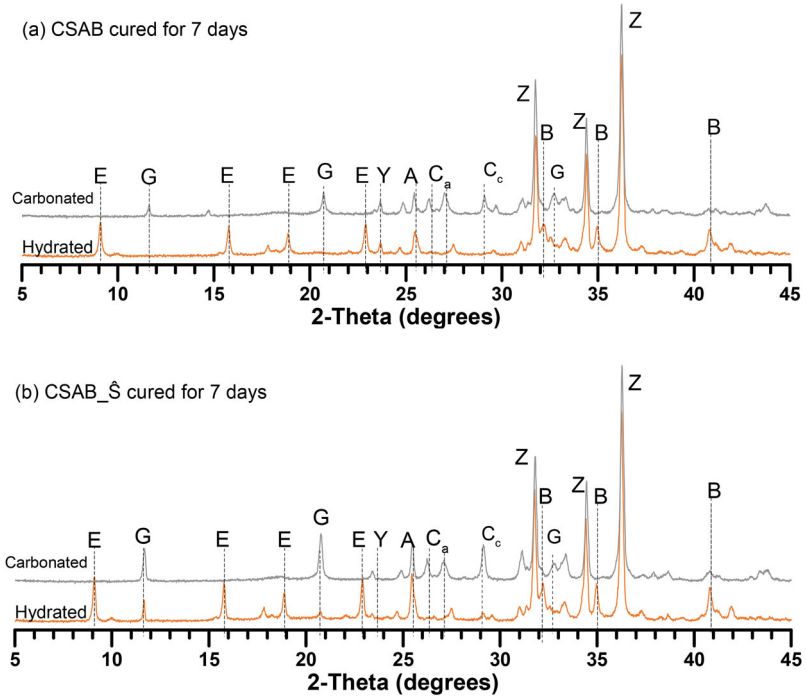

Figure 4. X-ray diffractograms of the hydrated (cured for 7 days) and carbonated (cured for 7 days followed by exposure to 3% CO_2 environment for 28 days) CSAB and CSAB blended with gypsum. [Note: E: Ettringite, G: Gypusm, Y: Ye'elimite, A: Anhydrite, C_a: Aragonite, C_c: Calcite; B: Belite]

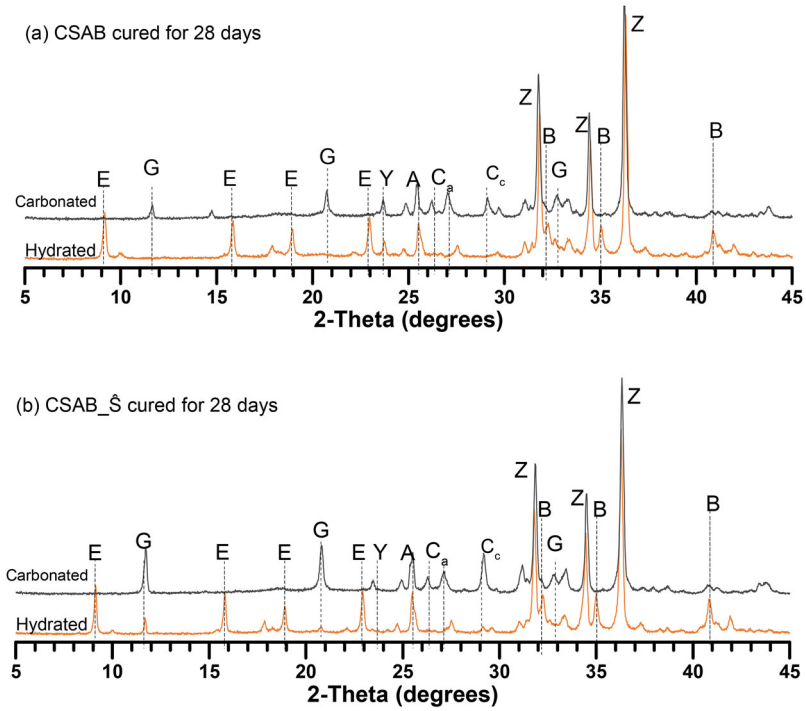

Figure 5. X-ray diffractograms of hydrated (cured for 28 days) and carbonated (cured for 28 days followed by exposure to 3% CO_2 environment for 28 days) CSAB and CSAB blended with gypsum. [Note: E: Ettringite, G: Gypusm, Y: Ye'elimite, A: Anhydrite, C_a: Aragonite, C_C: Calcite; B: Belite]

4.2.4. Modelling the carbonation of CSAB binders in GEMS

The changes in the hydrated phase assemblage were modelled using GEMS, as shown in Figure 7. The CSAB binder was considered to have only ye'elimite and calcium sulfate as the reactive phases to simulate the actual hydration process based on the XRD data (Figure 7a). The remaining phases were considered non-reactive. As the CSAB binder did not have sufficient source of sulfates to form ettringite completely (*M-value* < 2), GEMS predicted the formation of monosulfate (without CO_2 addition). In order to understand the phase changes with time or with the ingress of CO_2, incremental amounts of CO_2 were added to the reactants. Up on gradual addition of CO_2 to

Table 3. Carbonation-induced change in the hydrated phase composition of CSAB binders (in wt.%), as determined using QXRD.

	Hydrated sample (28 days)		Carbonated sample	
Phase	CSAB	CSAB_Ŝ	CSAB	CSAB_Ŝ
Ye'elimite	2.6	0.9	1.9	0.7
Anhydrite	3.5	5.5	3.3	7.1
Belite	16.8	15.4	0.8	6.6
Gypsum	0.1	2.9	10.4	21.0
Ettringite	29.4	32.0	0	0
Aragonite	0	0	11.5	10.7
Calcite	0	0	4.6	0.5
Amorphous content	43.4	40.4	65.8	51.3
Ferrite, mayenite, and dolomite	<2			

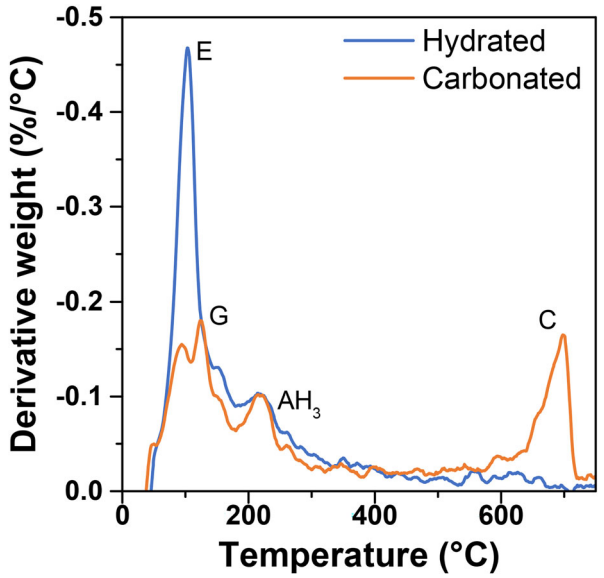

Figure 6. Derivative thermogravimetric analysis of carbonated and uncarbonated (28 days of hydration) CSAB samples. [Note: E: Ettringite, G: Gypusm, AH_3: Aluminium hydroxide, C: Calcium carbonate]

Table 4. Pore solution pH of the different CSAB binder systems.

Binder	Hydrated (1 day – Pore solution)	Hydrated (28 day – Powder)	Carbonated Powder
CSAB	12.05	11.06	8.79
CSAB_Ŝ	9.64	9.05	8.56

CSAB binder, the monosulfate phase initially converts into ettringite and monocarboaluminate [19]. After the consumption of monosulfate, the ettringite phase starts to decompose with the further increase in the concentration of CO_2. At about 10% addition of CO_2, there was a complete consumption of ettringite with the final products as gypsum, calcite and aluminium hydroxide. The stages of these phase changes are also reflected in measured pH of the pore solution. The initial pH of 11.68 drops to 9.87 after the consumption of monosulfate phase and plateaus till the complete consumption of ettringite, where it drops to less than 6. The change in the CSAB_Ŝ binder was similar to that in the CSAB binder, with ettringite decomposing first and its complete consumption at 8% CO_2 addition (Figure 7b). Although belite was found to be unhydrated, it was consumed when carbonated (Figures 4 and 5). Figure 7c shows the predicted phase assemblage considering the belite phase also to be reactive. In addition to the presence of calcite, gypsum and aluminium hydroxide, there was also the formation of amorphous silica. The presence of amorphous silica could also justify the high amounts of amorphous phases in the quantified phase assemblage (Table 3). The amount of CO_2 required for the complete transformation of the hydration products also increased significantly (from less than 10 to over 20 g/100g of binder). Further work needs to be done to understand the role of belite on the durability of the CSAB binder systems.

4.3. *Changes in the physical characteristic*

4.3.1. *Compressive strength*

The cement mortar cubes were exposed to two different environmental conditions of sealed and accelerated carbonation after an initial curing period of 28 days followed by the 7 days of conditioning (drying) similar to the prisms used for the measurement of depth of carbonation. One set of cubes were tested at 28 days and the compressive strength at 28 days was used to normalize the strength of the cubes under sealed and exposed conditions (Figure 8a). The compressive strength of PC continued to increase with age and there was a marginal increase on exposure to carbonation. In PC binders, carbonation has been reported to reduce the porosity and densify the pore structure [51]. Although the progression of the carbonation depth was less, the increase in compressive strength could be attributed to the densification of the pore structure. Whereas the strength of CSAB binders reduced after carbonation. Although the resistance to carbonation improved with the addition of gypsum, the reduction in compressive strength was more in the ettringite rich system (CSAB_ Ŝ).

4.3.2. *Pore structure features*

Oxygen permeability index (OPI) has been used to assess the quality of concretes. The OPI value can also be correlated with compressive strength. As the OPI value is based on the flow of oxygen (O_2), it also gives an indication of the changes in the pore structure features. The OPI values (Figure 8b) followed a similar trend to that of compressive strength for different binder systems. The OPI value of PC binder systems increased after carbonation, whereas it decreased for the CSAB binder systems. The reduction in compressive strength could be attributed to the increase in porosity. Further tests were performed using MIP to get a better understanding of the changes in the pore structure features. Figure 9 shows the change in the pore size distribution of CSAB binder systems before carbonation (at the ages of 7 days and 28 days) and post carbonation. The porosity of the hydrated matrix for both the binders decreased with age as a consequence of hydration. The reduction in

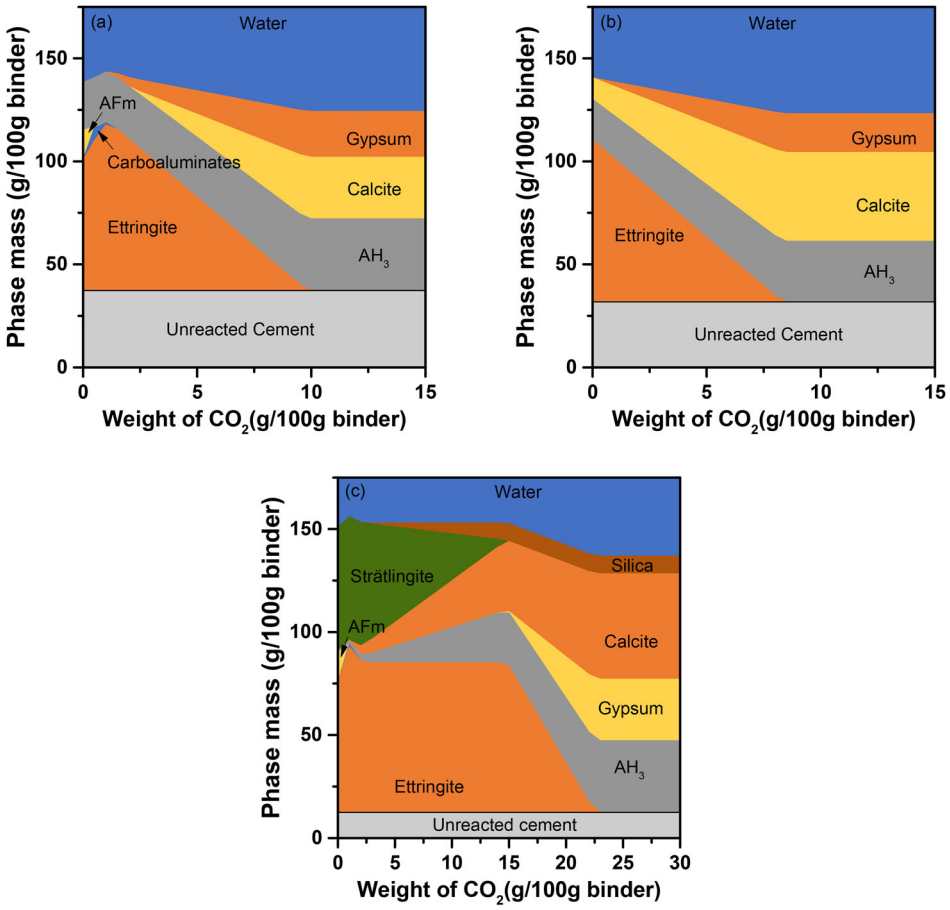

Figure 7. Changes in hydrated phase composition of CSAB cement on carbonation, modelled in GEMS for a) CSAB (belite considered as unreactive) b) CSAB_$\hat{S}$ (belite considered as unreactive) and c) CSAB (considering belite as reactive).

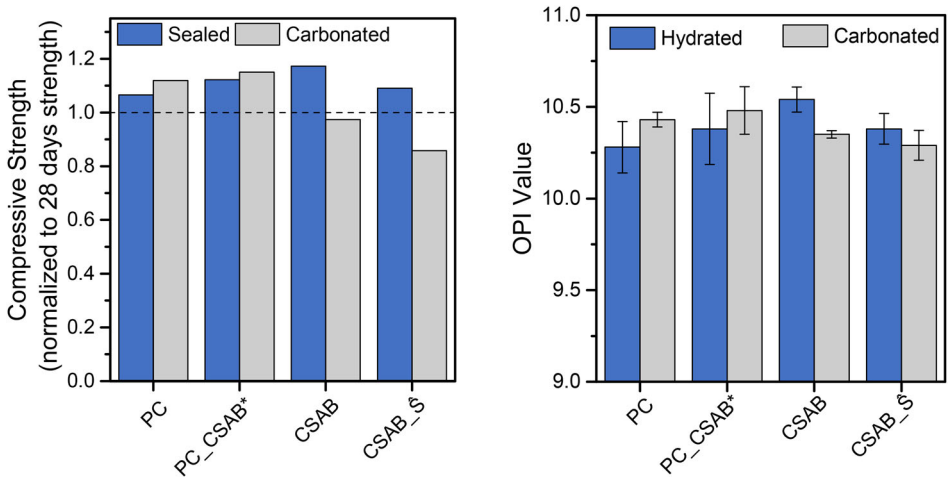

Figure 8. Left: Change in compressive strength due to carbonation (cement mortar specimen cured for 28 days, followed by 28 days of exposure to 3% CO_2); Right: OPI value of the different binders at 28 days and after exposure to 3% CO_2 for 28 days.

porosity was lesser in CSAB_$\hat{S}$ binder (Figure 9b) from 7 to 28 days when compared to CSAB binder. This could be attributed to the rapid ettringite formation at early ages. The reduced porosity and denser pore structure of CSAB_$\hat{S}$ binder could also be attributed to the improvement in the carbonation resistance than CSAB binder. The overall porosity of all CSAB binders increased with the coarsening of pores due to carbonation, as indicated by the increase in the cumulative pore volume and the rightward shift of critical pore size. The increase in porosity also seems to be more at higher replacement level of gypsum. A similar increase in porosity on carbonation for CSAB cement has been reported in the literature [19]. In CSAB cement, the decomposition of ettringite is

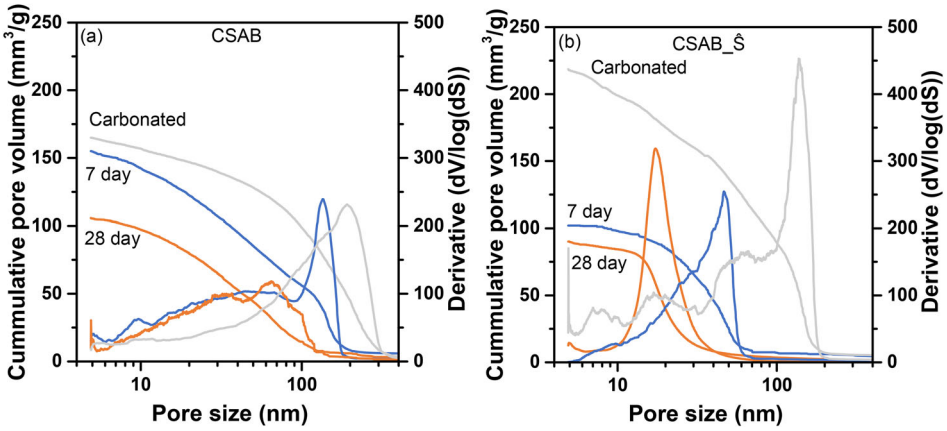

Figure 9. Pore size distributions of CSAB binders before and after carbonation.

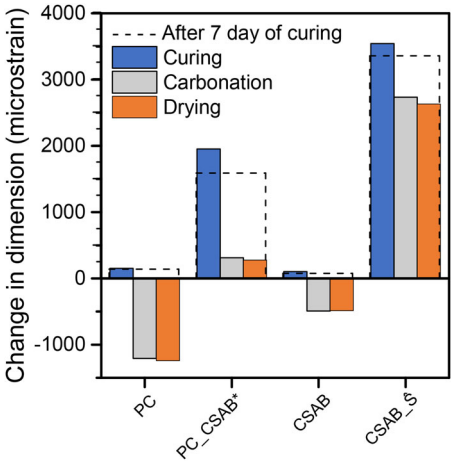

Figure 10. Effect of carbonation on the dimensional changes of CSAB binders.

accompanied with high amounts of water loss, which could lead to a significant increase in porosity. On the contrary, densification of pore structure is expected in PC on carbonation.

4.3.3. *Dimensional stability*

Dimensional changes of prismatic paste specimens were monitored during curing, drying, and carbonation as shown in Figure 10. The specimens were initially cured in saturated lime solution for 7 days and were exposed to three different environments: curing, drying (65% RH, atmospheric CO_2 conc.) and accelerated carbonation (3% CO_2 and 65% RH) till 28 days. The PC binder exhibited significant drying shrinkage compared to the CSAB binders. Hydrated PC binder with C-S-H gel as the main hydration product would be more susceptible to drying than ettringite in CSAB binder system, causing this difference [52,53]. Although there was a significant change in the porosity of CSAB binders, this did not affect the dimensional changes at the macroscale. The shrinkage due to drying and carbonation was similar in all CSAB binder systems (Figure 10). It can also be noted that both the expansive PC_CSAB and CSAB_$\hat{S}$ binder after 28 days of drying had net expansion.

4.4. *Rate of carbonation propagation in CSAB binder system*

The rate of ingress of CO_2 is represented as K_{CO2} (carbonation coefficient) and calculated based on the laws of diffusion. Tuutti's square root of time model is predominantly used to calculate K_{CO2} in PC binder systems, which is used as an indicator of the performance of concretes under carbonation [28]. The values of K_{CO2} for natural and accelerated carbonation were derived as the slope of linear function fitting the depth of carbonation against the square root of time. The carbonation coefficient for CSAB has been reported in the literature by directly using the carbonation depth at the different exposure durations [19]. However, in CSAB cement, using the square root of time was underestimating the carbonation depth at later ages (Figure 11). Rather, the progression of the carbonation front seems to deviate significantly at later stages. This behaviour in CSAB cement could be due to the progressive increase in porosity and coarsening of the pore structure with carbonation. Unlike the PC, where the carbonated layer can act as a barrier to restrict the further ingress of CO_2, in CSAB, the increase in porosity only facilitates further ingress of CO_2. The carbonation reaction in PC typically is accompanied by pore refinement and mass increase due to the conversion of calcium hydroxide into calcium carbonate. Whereas in CSAB binders, ettringite loses its bound water upon conversion to gypsum and aluminium hydroxide during drying. There was a significant reduction in the weight of powder samples due to carbonation in CSAB binders, unlike a weight increase in case of PC (Table 5). Also, the reaction of ettringite with CO_2 is the fastest among the hydrated phases (compared to portlandite and C-S-H). Hence, the reaction process in carbonation could be faster than the time taken for the diffusion of CO_2 [54]. The differences in the carbonation-induced changes of the binder systems are evident when the experimental data is compared against the model utilized for the PC binders (Figure 11). The model at later ages tends to underestimate the depth of carbonation when compared to the actual experimental data.

The scope of this study was limited to using cement paste and mortar for the estimation of carbonation depth. It is noted that the increase in binder's pore volume may

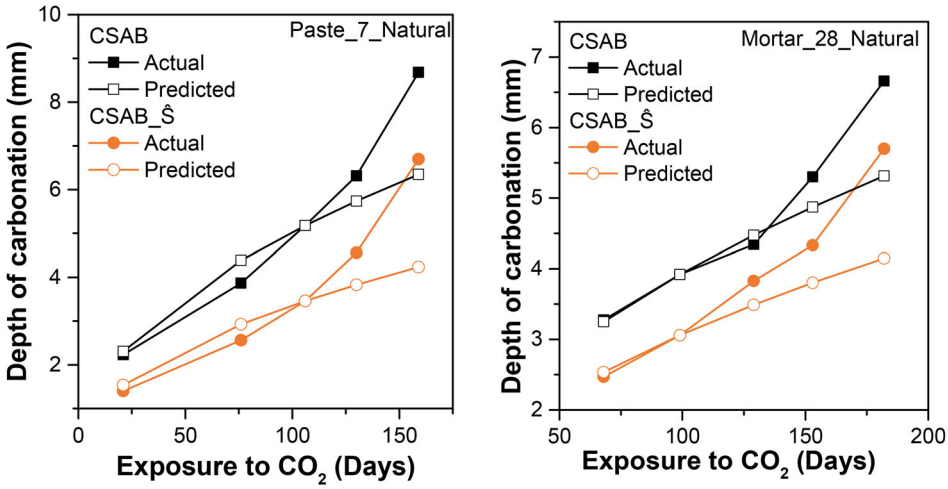

Figure 11. The depth of carbonation predicted using the Tuutti's model based on diffusion compared against experimental data.

Table 5. Changes observed in the mass, compressive strength and porosity of PC and CSAB binders after exposure to 3% CO_2 environment for 28 days (after 28 days of curing).

	CSAB	CSAB_Ŝ	PC	PC_CSAB*
Weight of powder sample	−3.6%	−6.9%	+8.6%	+7.3%
Compressive strength of cement mortar	−2.7%	−16.7%	+10.6%	+12.9%
Porosity	+36%	+53.3%	*	*

*Not determined.

not be as significant in concrete as observed in case of cement paste specimens. Also, the phase composition of CSAB binder must be considered while estimating the rate of carbonation in CSAB binders as the binder systems with a lower M-value or reactive belite would have a different hydrated phase assemblage affecting the rate of carbonation.

5. Conclusions

- CSAB binders used in this study exhibited poorer carbonation resistance than PC binders of similar compressive strength. Under accelerated carbonation conditions, when CSAB cement paste was almost fully carbonated (12.5 mm) by 28 days, the PC did not have any significant depth of carbonation.
- The carbonated CSAB binders had calcium sulfate (gypsum and anhydrite), calcium carbonate (calcite and aragonite) as the crystalline phases with aluminium hydroxide and other amorphous phase. The unhydrated belite was also observed to be consumed on carbonation.
- The addition of calcium sulfate to CSAB helped improve the carbonation resistance; however, it led to reduced compressive strength post carbonation.
- The porosity of CSAB binders increased upon carbonation, thus facilitating further ingress of CO_2. The square root of time model for estimating the carbonation depth underestimated the values in CSAB binders at later ages.

Acknowledgement

The first author would like to acknowledge the doctoral scholarship received from the Ministry of Education (MoE), India. All authors would like to acknowledge the resources provided by the Department of Civil Engineering at the Indian Institute of Technology (IIT) Madras towards the usage of experimental facilities in this study. The last author is also grateful for the financial support from the New Faculty Seed Grant by Industrial Consultancy and Sponsored Research (ICSR) centre at IIT Madras. The Centre of Excellence on Technologies for Low Carbon and Lean Construction (TLC2) at IIT Madras is also gratefully acknowledged.

Disclosure statement

No potential conflict of interest was reported by the author(s).

Funding

This work was supported by Ministry of Education, India.

References

[1] Chaunsali P, Kumar SV. Calcium sulfoaluminate-belite cements: opportunities and challenges. Indian Concr J. 2020;94(2):18–25.
[2] Gartner E. Industrially interesting approaches to 'low-CO2' cements. Cem Concr Res. 2004;34(9):1489–1498. doi: 10.1016/j.cemconres.2004.01.021.
[3] Gartner E, Sui T. Alternative cement clinkers. Cem Concr Res. 2016;114:27–39. doi: 10.1016/j.cemconres.2017.02.002.

[4] Juenger MCG, Winnefeld F, Provis JL, et al. Advances in alternative cementitious binders. Cem Concr Res. 2011;41(12):1232–1243. doi: 10.1016/j.cemconres.2010.11.012.
[5] Gettu R, Patel A, Rathi V, et al. Influence of supplementary cementitious materials on the sustainability parameters of cements and concretes in the Indian context. Mater Struct. 2019;52(1):1–11. doi: 10.1617/s11527-019-1321-5.
[6] Scrivener KL, John VM, Gartner EM. Eco-efficient cements: potential economically viable solutions for a low-CO2 cement-based materials industry. Cem Concr Res. 2018;114(June):2–26. doi: 10.1016/j.cemconres.2018.03.015.
[7] Sharp JH, Lawrence CD, Yang R. Calcium sulfoaluminate cements—low-energy cements, special cements or what? Adv Cem Res. 1999;11(1):3–13. doi: 10.1680/adcr.1999.11.1.3.
[8] Bullerjahn F, Boehm-Courjault E, Zajac M, et al. Hydration reactions and stages of clinker composed mainly of stoichiometric ye'elimite. Cem Concr Res. 2019;116:120–133. doi: 10.1016/j.cemconres.2018.10.023.
[9] Ben Haha M, Winnefeld F, Pisch A. Advances in understanding ye'elimite-rich cements. Cem Concr Res. 2019;123(May):105778. doi: 10.1016/j.cemconres.2019.105778.
[10] Zhang L, Glasser FP. Hydration of calcium sulfoaluminate cement at less than 24 h. Adv Cem Res. 2002;14(4):141–155. doi: 10.1680/adcr.2002.14.4.141.
[11] Bernardo G, Telesca A, Valenti GL. A porosimetric study of calcium sulfoaluminate cement pastes cured at early ages. Cem Concr Res. 2006;36(6):1042–1047. doi: 10.1016/j.cemconres.2006.02.014.
[12] Gastaldi D, Canonico F, Capelli L, et al. Hydraulic behaviour of calcium sulfoaluminate cement alone and in mixture with Portland cement. 13th Int Congr Chem Cem. 2011:1–7.
[13] Wang P, Li N, Xu L. Hydration evolution and compressive strength of calcium sulphoaluminate cement constantly cured over the temperature range of 0 to 80 °C. Cem Concr Res. 2017;100(July):203–213. doi: 10.1016/j.cemconres.2017.05.025.
[14] Winnefeld F, Lothenbach B. Hydration of calcium sulfoaluminate cements - Experimental findings and thermodynamic modelling. Cem Concr Res. 2010;40(8):1239–1247. doi: 10.1016/j.cemconres.2009.08.014.
[15] Carsana M, Canonico F, Bertolini L. Corrosion resistance of steel embedded in sulfoaluminate-based binders. Cem Concr Compos. 2018;88:211–219. doi: 10.1016/j.cemconcomp.2018.01.014.
[16] Ma J, Wang H, Yu Z, et al. A systematic review on durability of calcium sulphoaluminate cement-based materials in chloride environment. J Sustain Cem Mater. 2023;12(6):687–698. doi: 10.1080/21650373.2022.2113569.
[17] Moffatt EG, Thomas MDA. Durability of rapid-strength concrete produced with ettringite-based binders. ACI Mater J. 2018;115(1):105–115. doi: 10.14359/51701006.
[18] Bertola F, Gastaldi D, Irico S, et al. Influence of the amount of calcium sulfate on physical/mineralogical properties and carbonation resistance of CSA-based cements. Cem Concr Res. 2022;151:106634. doi: 10.1016/j.cemconres.2021.106634.
[19] Hargis CW, Lothenbach B, Müller CJ, et al. Carbonation of calcium sulfoaluminate mortars. Cem Concr Compos. 2017;80(October):123–134. doi: 10.1016/j.cemconcomp.2017.03.003.
[20] Ioannou S, Paine K, Reig L, et al. Performance characteristics of concrete based on a ternary calcium sulfoaluminate-anhydrite-fly ash cement. Cem Concr Compos. 2015;55:196–204. doi: 10.1016/j.cemconcomp.2014.08.009.
[21] Quillin K. Performance of belite-sulfoaluminate cements. Cem Concr Res. 2001;31(9):1341–1349. doi: 10.1016/S0008-8846(01)00543-9.
[22] Sherman N, Beretka J, Santoro L, et al. Long-term behaviour of hydraulic binders based on calcium sulfoaluminate and calcium sulfosilicate. Cem Concr Res. 1995;25(1):113–126. doi: 10.1016/0008-8846(94)00119-J.
[23] Zhang L, Glasser FP. Investigation of the microstructure and carbonation of CS\barA-based concretes removed from service. Cem Concr Res. 2005;35(12):2252–2260. doi: 10.1016/j.cemconres.2004.08.007.
[24] Damion T, Cepuritis R, Chaunsali P. Sulfuric acid and citric acid attack of calcium sulfoaluminate-based binders. Cem Concr Compos. 2022;130:104524. doi: 10.1016/j.cemconcomp.2022.104524.
[25] Damion T, Chaunsali P. Evaluating acid resistance of Portland cement, calcium aluminate cement, and calcium sulfoaluminate based cement using acid neutralisation. Cem Concr Res. 2022;162(October):107000. doi: 10.2139/ssrn.4165828.
[26] Rathnarajan S, Dhanya BS, Pillai RG, et al. Carbonation model for concretes with fly ash, slag, and limestone calcined clay - using accelerated and five - year natural exposure data. Cem Concr Compos. 2022;126:104329. doi: 10.1016/j.cemconcomp.2021.104329.
[27] Verbeck GJ. Carbonation of hydrated Portland cement. West Conshohocken, PA, USA ASTM Int. 1958:17–36.
[28] Kyösti T. Corrosion of steel in concrete, Swedish Cement and Concrete Research Institute, Stockholm; 1982.
[29] Dhanya BS, Santhanam M. Point of view performance specifications for concrete construction in India: are we ready. Indian Concr J. 2015;87:36–43.
[30] Parrott LJ. Factors influencing relative humidity in concrete. Mag Concr Res. 1991;43(154):45–52. doi: 10.1680/macr.1991.43.154.45.
[31] Šavija B, Luković M. Carbonation of cement paste: understanding, challenges, and opportunities. Constr Build Mater. 2016;117:285–301. doi: 10.1016/j.conbuildmat.2016.04.138.
[32] Duan P, Chen W, Ma J, et al. Influence of layered double hydroxides on microstructure and carbonation resistance of sulphoaluminate cement concrete. Constr Build Mater. 2013;48:601–609. doi: 10.1016/j.conbuildmat.2013.07.049.
[33] Mechling J-M, Lecomte A, Roux A, et al. Sulfoaluminate cement behaviours in carbon dioxide, warm and moist environments. Adv Cem Res. 2014;26(1):52–61. doi: 10.1680/adcr.12.00070.
[34] Moffatt EG, Thomas MDA. Effect of carbonation on the durability and mechanical performance of ettringite-based binders. ACI Mater J. 2019;116(1):95–102. doi: 10.14359/51710965.
[35] Vasudevan D, Trejo D. Suitability of CPC-18 and carbonation of specialty cementitious systems. ACI Mater J. 2022;119(3):79–90. doi: 10.14359/51734609.
[36] Papadakis VG. Effect of supplementary cementing materials on concrete resistance against carbonation and chloride ingress. Cem Concr Res. 2000;30(2):291–299. doi: 10.1016/S0008-8846(99)00249-5.
[37] Ioannou S, Paine KA. Strength and durability of calcium sulfoaluminate based concretes. IC-NOCMAT 2010, Int. Conf. Non-Conventional Mater. Technol. Ecol. Mater. Technol. Sustain. Build. 2010.
[38] Chaunsali P, Mondal P. Hydration and early-age expansion of calcium sulfoaluminate cement based-binders: Experiments and … hydration and early-age expansion of calcium sulfoaluminate cement-based binders. J Sustain Cem Mater. 2015;5(4):259–267. doi: 10.1080/21650373.2015.1060184.

[39] Shenbagam VK, Cepuritis R, Chaunsali P. Influence of exposure conditions on expansion characteristics of lime-rich calcium sulfoaluminate-belite blended cement. Cem Concr Compos. 2021;118:103932. doi: 10.1016/j.cemconcomp.2021.103932.
[40] Shenbagam VK, Chaunsali P. Influence of calcium hydroxide and calcium sulfate on early-age properties of non-expansive calcium sulfoaluminate belite cement. Cem Concr Compos. 2022;128(February):104444. doi: 10.1016/j.cemconcomp.2022.104444.
[41] Alexander M, Ballim Y, Mackechnie JM. Durability index testing procedure manual. Res Monogr No.4. 2018:29.
[42] Barneyback RS, Diamond S. Expression and analysis of pore fluids from hardened cement pastes and mortars. Am Concr Institute, ACI Spec Publ. 2008;SP-249:55–65.
[43] Kulik D. "GEM-Selektor v.3." *PSI, Villigne, Switzerland*;2002. https://gems.web.psi.ch/
[44] Kulik DA, Wagner T, Dmytrieva SV, et al. GEM-Selektor geochemical modeling package: revised algorithm and GEMS3K numerical kernel for coupled simulation codes. Comput Geosci. 2012;17(1):1–24. doi: 10.1007/s10596-012-9310-6.
[45] Wagner T, Kulik DA, Hingerl FF, et al. Gem-selektor geochemical modeling package: TSolMod library and data interface for multicomponent phase models. Can Mineral. 2012;50(5):1173–1195. doi: 10.3749/canmin.50.5.1173.
[46] Lothenbach B, Kulik DA, Matschei T, et al. Cemdata18: a chemical thermodynamic database for hydrated Portland cements and alkali-activated materials. Cem Concr Res. 2019;115:472–506. doi: 10.1016/j.cemconres.2018.04.018.
[47] Rodriguez-Navarro, C., Cazalla, O., Elert, K., & Sebastian, E. (2002). Liesegang pattern development in carbonating traditional lime mortars. Proceedings of the Royal Society of London. Series A: Mathematical, Physical and Engineering Sciences, 458(2025), 2261-2273. doi: 10.1098/rspa.2002.0975.
[48] Telesca A, Marroccoli M, Pace ML, et al. A hydration study of various calcium sulfoaluminate cements. Cem Concr Compos. 2014;53:224–232. doi: 10.1016/j.cemconcomp.2014.07.002.
[49] Seo J, Kim S, Park S, et al. Carbonation of calcium sulfoaluminate cement blended with blast furnace slag. Cem Concr Compos. 2021;118(January):103918. doi: 10.1016/j.cemconcomp.2020.103918.
[50] Wang W, Wei X, Cai X, et al. Mechanical and microstructural characteristics of calcium sulfoaluminate cement exposed to early-age carbonation curing. Materials (Basel). 2021;14(13):3515. doi: 10.3390/ma14133515.
[51] Ngala VT, Page CL. Effects of carbonation on pore structure and diffusional properties of hydrated cement pastes. Cem Concr Res. 1997;27(7):995–1007. doi: 10.1016/S0008-8846(97)00102-6.
[52] Glasser FP, Zhang L. High-performance cement matrices based on calcium sulfoaluminate-belite compositions. Cem Concr Res. 2001;31(12):1881–1886. doi: 10.1016/S0008-8846(01)00649-4.
[53] Sirtoli D, Wyrzykowski M, Riva P, et al. Shrinkage and creep of high-performance concrete based on calcium sulfoaluminate cement. Cem Concr Compos. 2019;98:61–73. doi: 10.1016/j.cemconcomp.2019.02.006.
[54] Castellote M, Andrade C. Modelling the carbonation of cementitious matrixes by means of the unreacted-core model, UR-CORE. Cem Concr Res. 2008;38(12):1374–1384. doi: 10.1016/j.cemconres.2008.07.004.